60 nJ, 95 fs environmentally stable Er-doped fiber laser system

Peng Luo (罗 鹏)[1], Qiang Hao (郝 强)[1,*], Hanmei Fu (付寒梅)[1], and Heping Zeng (曾和平)[1,2]

[1]*Shanghai Key Laboratory of Modern Optical System, and Engineering Research Center of Optical Instrument and System, Ministry of Education, School of Optical Electrical and Computer Engineering, University of Shanghai for Science and Technology, Shanghai 200093, China*

[2]*State Key Laboratory of Precision Spectroscopy, East China Normal University, Shanghai 200062, China*

**Corresponding author: qianghao@usst.edu.cn*

Received January 24, 2019; accepted March 8, 2019; posted online May 29, 2019

We demonstrate here an environmentally stable and extremely compactable Er-doped fiber laser system capable of delivering sub-100-fs temporal duration and tens of nanojoules at a repetition rate of 10 MHz. This laser source employs a semiconductor saturable absorber mirror mode-locked soliton laser to generate seed pulses. A single-mode-fiber amplifier and a double-cladding-fiber amplifier (both with double-pass configuration) are bridged by a divider and used to manage the dispersion map and boost the soliton pulses. By using 64 replicas, pulses with as high as 60 nJ energy within 95 fs duration are obtained at 10 MHz, corresponding to 600 kW peak power.

OCIS codes: 140.3500, 140.3510, 140.4480, 140.7090.
doi: 10.3788/COL201917.061401.

Ultrafast laser pulses at 1.55 μm have gained much attraction for wide applications in optical communications, medical diagnosing, material processing, precision metrology, and nonlinear optics[1–3]. Environmentally stable ultrafast Er-doped fiber lasers have emerged as the most commonly used lasers and exhibited several outstanding superiorities, such as compact size, being free of alignment, robustness, and low cost. To enable the above mainstream applications, the developing trends of ultrafast lasers are: firstly, higher pulse energy together with shorter pulse duration; secondly, long-term environmental stability.

Soliton and stretch-pulse lasers at 1.55 μm have been fully investigated[4–10]. Recently, the developments of ultrafast Er-doped fiber laser oscillators (EDFOs) were reviewed by Brida *et al.*[11], and a comprehensive study of similaritons in Er-doped fiber lasers was reviewed by Chong *et al.*[12]. To increase the pulse energy, a dissipative soliton (DS), which generates highly chirped pulses from a chirped-pulse oscillator (CPO), is proposed and widely investigated. Normally, the DS laser was conducted by using tens of meters of normal dispersion fiber so as to decrease the pulse repetition rate and thereupon increase the pulse energy. The drawback of doing so is that it inevitably introduces excessive nonlinear phase shifts and higher-order dispersion, which are hardly compensated by the extra-cavity linear dispersion delay line. Up to now, the highest compressed pulse energies and the corresponding pulse durations (uncompressed pulse energies and pulse durations) from ultrafast CPOs at 1.55 μm were 7.5 nJ and 75 fs (10 nJ and 4.0 ps)[13], 6.4 nJ and 750 fs (20 nJ and 53 ps)[14], 11.9 nJ and 156 fs (33 nJ and 3.0 ps)[15], 27.2 nJ and 700 fs (38 nJ and 10.5 ps)[16], respectively.

Er-doped fiber laser amplifiers (EDFAs) are widely used for power amplification at 1.55 μm. When a pulse with 10 kW peak power is restricted in fiber with a 10 μm diameter, nonlinear effects arise, and pulse distortion happens. Therefore, state-of-the-art experiments using fiber-based chirped-pulse amplification (FCPA) technology, together with a large-mode-area (LMA) fiber, or even a rod-type fiber, mitigate the nonlinearity in power amplification. To date, the highest compressed pulse energies and the corresponding pulse durations (uncompressed pulse energies and pulse durations) from FCPAs at 1.55 μm were 16 nJ and 450 fs (64 nJ and 40 ps)[17], 45 nJ and 175 fs (80 nJ and 7.0 ps)[18], 71 nJ and 876 fs (118 nJ and 20 ps)[19], 157 nJ and 850 fs (228 nJ and ∼ps)[20], 173 nJ and 835 fs (325 nJ and unmentioned)[21], and 310 nJ and 570 fs (1.37 μJ and 100 ps)[22]. Due to the accumulated nonlinear phase shift and the mismatch of high-order dispersion between the stretchers and the compressors, the amplified pulses are hardly compressed to its transform limit; meanwhile, partial energy locates in the pedestal, and thus the actual pulse energy has an inevitable discount. Furthermore, the poor efficiency of the grating compressor is another obstacle for both DS and FCPA. The orange and blue dot lines in Fig. 1 represent the pulse duration-energy limits for CPO and chirped pulse amplification (CPA) technology at 1.55 μm. It can be seen that EDFOs and EDFAs have not yet reconciled the demands of ultrashort pulses with both short temporal duration (<100 fs) and high peak power (>500 kW).

Environmental stability is another key issue for ultrafast fiber lasers. Most of the above mentioned EDFOs and EDFAs are based on non-polarization-maintaining (PM) single-mode fibers (SMFs) or LMA fibers; thus, the laser system is not environmentally stable. The environmentally unstable and stable laser systems are shown as hollow and solid patterns in Fig. 1, respectively. As far as we know, all of the results with above 10 nJ pulse energy

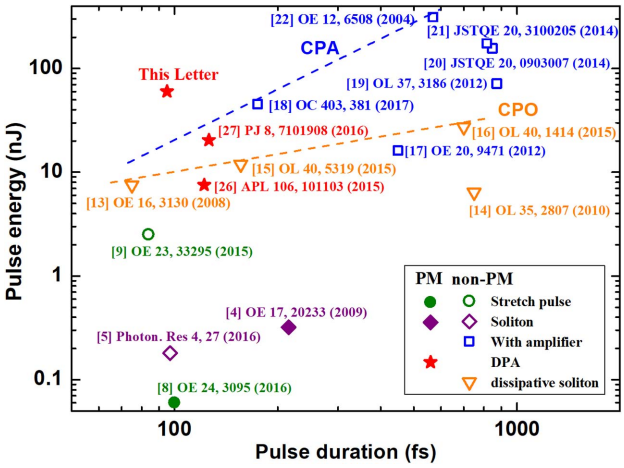

Fig. 1. Overview of the compressed pulse energy versus the corresponding pulse duration of the EDFOs and EDFAs. Environmentally stable laser configurations are marked as solid patterns, and non-PM laser configurations are marked as hollow patterns.

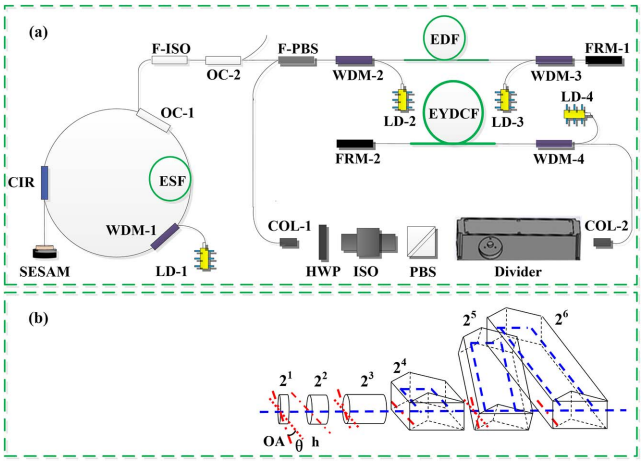

Fig. 2. (a) Laser system setup. LD-1, LD-2, and LD-3, single-mode fiber coupled laser diode with a maximum output power of 400 mW at 976 nm; ESF, Er-doped single-mode fiber with negative GVD; CIR, circulator; WDM-1, WDM-2, WDM-3, and WDM-4, wavelength division multiplexer; OC-1 and OC-2, fiber couplers with 30:70 and 10:90 splitting ratio, respectively; F-ISO, fiber-coupled isolator; F-PBS, fiber-coupled polarization beam splitter; EDF, Er-doped single-mode fiber with positive GVD; FRM-1 and FRM-2, Faraday rotation mirror; COL-1, input collimator; COL-2, output collimator; HWP, half-wave plate; ISO, isolator; PBS, polarization beam splitter cube; LD-4, laser diode with 9 W output power; EYDCF, 12/130 Er–Yb codoped double-clad fiber with numerical aperture of 0.2 for the fiber core and 0.46 for the cladding. (b) Optical alignment of the ×64 divider, with the inline YVO_4-based stages as well as the PBS-based stages. N in 2^N represents the stage order. The red dash line OA, red dot line h, and θ represent the crystal optical axis, horizontal line, and angle between them, respectively.

achieved by CPO and CPA architectures have inherent environmental instabilities.

Divided-pulse amplification (DPA) is an effective method for ultrashort pulse amplification at 1.06 and 1.55 μm[23–27]. A single seed pulse is temporally divided into 2^N time-delayed replicas, where N is the stage number of the divider. The polarization of odd-N pulses and even-N pulses are perpendicular to each other. With a specially designed fiber amplifier, each of these replicas experiences identical laser gain and possesses the same temporal and spectral shape, thus ensuring high-efficiency recombination. As shown in Fig. 1, two previous results marked as five-point stars approach the CPO and CPA duration-energy limits. In this Letter, we report a compactable Er-doped fiber laser system capable of delivering as high as 60 nJ pulse energy within sub-100-fs temporal duration, corresponding to 600 kW peak power. To the best of our knowledge, this is the highest peak power from an environmentally stable Er-doped fiber laser system.

Our previous experiments applied stretched-pulse fiber oscillators at 80 MHz repetition rate, utilizing non-PM fibers[26,27]. To improve the environmental stability and pulse energy, a semiconductor saturable absorber mirror (SESAM) mode-locked all-PM fiber laser oscillator operating at 10 MHz repetition rate is used as the seed laser. The schematic of the proposed Er-doped fiber laser system is depicted in Fig. 2. The current soliton laser oscillator is constructed by 1.5 m Er-doped single-mode fiber with negative group velocity dispersion (GVD) (ESF, Nufern) and 18.5 m SMF. Considering the GVDs of the ESF and SMF are −20.5 and −22.0 fs^2/mm, respectively, the net cavity dispersion is calculated to be −0.44 ps^2. A 976 nm laser diode delivers up to 400 mW pumping power to the gain fiber through wavelength division multiplexing. The 30% port of a coupler with 30:70 splitting ratio acts as the output port.

The threshold pumping power is measured to be 44.6 mW. The fundamental repetition rate remains stable (without mode jump) in a certain range of pumping power. As the pumping power changes from 43.8 to 46.8 mW, the spectral width of the pulse increases from 2.6 to 3.6 nm. Figures 3(a) and 3(b) show the spectral and temporal characters of the soliton laser. The spectrum and the autocorrelation (AC) trace are recorded by a spectrum analyzer and a pulse autocorrelator, respectively.

A double-pass SMF amplifier is used to pre-amplify and positively pre-chirp the seed pulse. Afterwards, the pre-chirped pulse is divided by a hybrid divider so as to extract more energy and manage the nonlinearity in the main amplifier. As depicted in Fig. 2(b), three YVO_4 crystals 2^1, 2^2, and 2^3 with lengths of 10, 20, and 40 mm divide the initial pulse into eight replicas. In the consideration of the expensive price, optical quality, and composability, bulk polarization beam splitters (PBSs) are used as the subsequent 2^4, 2^5, and 2^6 dividers. The optical axes (OAs) of 2^1 and 2^3 YVO_4-based dividers and 2^5 PBS-based divider orient at an angle of 45° to the horizontal plane. Thus, an incident pulse with horizontal polarization can be divided into 64 replicas.

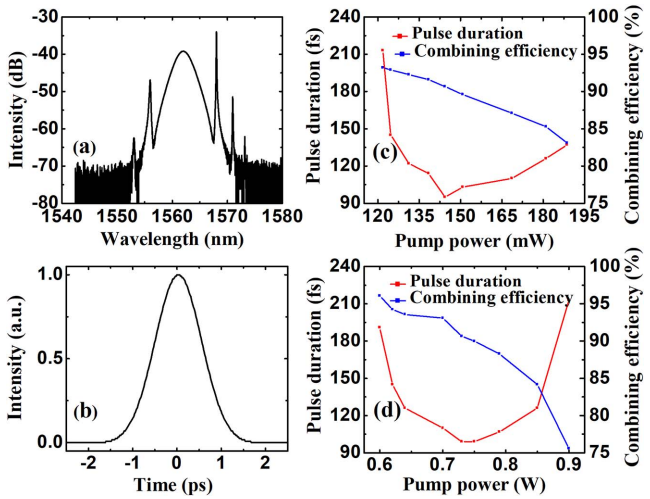

Fig. 3. (a) Spectral curve and (b) AC trace of the seed pulse at 10 MHz repetition rate. Pulse durations (red square curve) and combining efficiencies (blue square curve) as functions of the pumping power of the (c) pre-amplifier and (d) main amplifier, respectively.

The main amplifier applies the same double-pass configuration as the pre-amplifier. The double-pass configuration with the combination of a fiber-based PBS (F-PBS) and a Faraday rotation mirror (FRM) not only can suppress the amplified spontaneous emission (ASE) noise in the fiber amplifier by double-passing the active fiber, but also can rotate the polarization of the incident pulse by 90° to cancel all birefringence influence (including temperature, pressure, humidity, and vibration) in fibers. In the main amplifier, replicas are amplified in a segment of Er–Yb codoped double-clad fiber (EYDCF), reflected and polarization-rotated 90° by FRM-2, then amplified in the same EYDCF once more, and finally recombined in the same divider (but in an opposite direction). It is worth noting that the excessive nonlinear effect accumulation would badly distort the pulse and discount the combining efficiency. It has been theoretically revealed that, with the divided-pulse nonlinear amplification and compression simultaneously taking place, there exists an equilibrium position that can not only restrict excessive nonlinear effects to ensure high-quality temporal integrity, but also produce sufficient optical nonlinearity to broaden the spectrum to support <100 fs pulse duration[27]. From the current experiment (soliton pulses with 10 MHz repetition rate) point of view, the lengths of SMF and Er-doped single-mode fiber with positive GVD (EDF) in the pre-amplifier are optimized to 130 and 165 cm, and the lengths of the SMF and EYDCF in the main amplifier are optimized to 71 and 112 cm, respectively.

To investigate the DPA and compression at 10 MHz repetition rate, the divider firstly operates with eight replicas. Figures 3(c) and 3(d) record the pulse duration as well as the combining efficiencies as functions of pumping power in the pre-amplifier and main amplifier, respectively. Obviously, the shortest pulse duration is achieved at 144 mW pumping power in the pre-amplifier and 0.73 W pumping power in the main amplifier. Increasing or decreasing the pumping power will both stretch the pulse duration. In Fig. 3(c), the combining efficiency starts at a value of 93.2% and degrades to 83.1% as the pumping power of the pre-amplifier increases from 123 to 190 mW. As the pumping power increases, the spectral width of the amplified pulse increases, owing to self-phase modulation, and the pulse temporal duration decreases under the influence of dispersion. With lower pumping power, the newly generated spectral components maintain good coherence and do not obviously degrade the combining efficiency. The imperfect combining efficiency can be partially attributed to the unequal pulse energy of replicas and the consequent accumulated phase difference. With higher pumping power, higher nonlinearity and the accordingly larger different phase shift make the newly generated spectral components hardly recombine. As shown in Fig. 3(d), the shortest pulse duration can be achieved by adjusting the pumping power of the main amplifier. The shortest pulse duration is 95 fs with 0.73 W pumping power. The combining efficiency starts at a value of 96.0% and degrades to 75.2% as the pumping power increases from 0.6 to 0.9 W.

To further extract more energy from the main amplifier, we apply 64 replicas. The energy consistency of each replica as well as the coupling efficiency between the input collimator (COL-1) and the output collimator (COL-2) is closely related to the alignment of PBS-based dividers. Owing to the differential GVD between two orthogonal polarizations in the divider (a typical value of 40 fs^2/mm for YVO_4 and 24 fs^2/mm for the fused-silica PBS), the fiber length in the pre-amplifier and main amplifier are adjusted carefully. The lengths of SMF and EDF in the pre-amplifier are optimized to 104 and 178 cm in the pre-amplifier, and those of the SMF and EYDCF in the main amplifier are optimized to 66 and 97 cm, respectively. Besides, to avoid fiber damage, the splicing point at the common port of the combiner and the EYDCF has been well treated for heat dissipation.

Figures 4(a) and 4(b) show the pulse characters of the main amplifier. With 8.3 W pumping power, 600 mW average power is achieved, corresponding to 60 nJ pulse energy. The available shortest pulse duration is 95 fs, which is marked as the top five-point star in Fig. 1. A little bit of a pulse pedestal could be distinguished on the AC trace. A limitation in further increasing the output power is the self-oscillation in the main amplifier. As the average power exceeds 650 mW, CW spectral peaks happen at 1550 nm, and about 10% of power fluctuations can be observed.

A periodically poled lithium niobate (PPLN) crystal with 20.9 μm poling period and 0.45 mm length is used for frequency doubling to check pulse peak power at room temperature. The spectrum and the corresponding AC trace of the frequency-doubled pulses at 785 nm are shown in Figs. 4(c) and 4(d). By optimizing the pumping power of the main amplifier, a better equilibrium between higher-order dispersion and nonlinear phase shift for frequency doubling

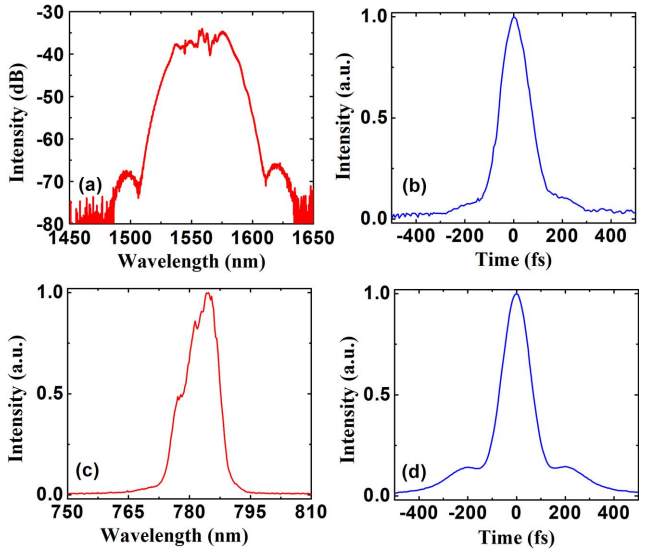

Fig. 4. (a) Spectral and (b) temporal characters of the amplified pulse with 64 replicas. (c) Spectral and (d) temporal characters of the frequency-doubled pulse.

could be found[28]. As a result, a pedestal-free AC trace (compared with its fundamental counterpart) of 785 nm pulse is obtained. To avoid optical damage on PPLN, the incident laser is kept below 500 mW. With 438 mW incident power at 1570 nm, an average power of 162 mW is achieved, corresponding to 37% conversion efficiency.

In conclusion, we propose an environmentally stable Er fiber laser system capable of delivering 60 nJ energy in <100 fs duration at 10 MHz repetition rate. An all-PM fiber soliton laser oscillator provides the seed pulses for the following cascaded fiber amplifier. A two-stage fiber amplifier bridged by a pulse divider performs divided-pulse nonlinear amplification and compression. By optimizing the pumping power in the pre-amplifier and main amplifier, the shortest pulse duration achieved is 95 fs. Although the YVO_4 and PBS dividers as well as the bulk optics seem to break the all-fiber concept, such a device can be designed with a fiber-coupled device and compacted in a size of about 4 cm × 4 cm × 25 cm (irregular shape). With 64 replicas, the coupling efficiency between COL-1 and COL-2 is as much as 80%. Therefore, such a high-energy fiber laser system with an environmentally stable configuration is a potential laser source for the applications in infrared spectroscopy, three-photon microscopy, pump–probe spectroscopy, etc.

This work was supported by the National Key R&D Program of China (No. 2018YFB0407100).

References

1. H. Haus and W. S. Wong, Rev. Mod. Phys. **68**, 423 (1996).
2. R. R. Gattass and E. Mazur, Nat. Photon. **2**, 219 (2008).
3. B. R. Washburn, S. A. Diddams, N. R. Newbury, J. W. Nicholson, M. F. Yan, and C. G. Jorgensen, Opt. Lett. **29**, 250 (2004).
4. Y. Senoo, N. Nishizawa, Y. Sakakibara, K. Sumimura, E. Itoga, H. Kataura, and K. Itoh, Opt. Express **17**, 20233 (2009).
5. J. Zhang, Z. Kong, Y. Liu, A. Wang, and Z. Zhang, Photon. Res. **4**, 27 (2016).
6. J. Shi and W. Zhou, Chin. Opt. Lett. **16**, 031404 (2018).
7. Z. Dong, R. Xu, W. Zhang, H. Guoyu, L. Hua, J. Tian, and Y. Song, Chin. Opt. Lett. **16**, 081402 (2018).
8. N. Kuse, J. Jiang, C.-C. Lee, T. R. Schibli, and M. E. Fermann, Opt. Express **24**, 3095 (2016).
9. D. A. Dvoretskiy, V. A. Lazarev, V. S. Voropaev, Z. N. Rodnova, S. G. Sazonkin, S. O. Leonov, A. B. Pnev, V. E. Karasik, and A. A. Krylov, Opt. Express **23**, 33295 (2015).
10. H. Ahmad, S. I. Ooi, M. Z. A. Razak, S. R. Azzuhri, A. A. Jasim, K. Thambiratnam, M. F. Ismail, and M. A. Ismail, Chin. Opt. Lett. **15**, 051402 (2017).
11. D. Brida, G. Krauss, A. Sell, and A. Leitenstorfer, Laser Photon. Rev. **8**, 409 (2014).
12. A. Chong, L. G. Wright, and F. W. Wise, Rep. Prog. Phys. **78**, 113901 (2015).
13. A. Ruehl, V. Kuhn, D. Wandt, and D. Kracht, Opt. Express **16**, 3130 (2008).
14. N. B. Chichkov, K. Hausmann, D. Wandt, U. Morgner, J. Neumann, and D. Kracht, Opt. Lett. **35**, 2807 (2010).
15. K. Chu, H. Jiang, and S. Yang, Opt. Lett. **40**, 5319 (2015).
16. M. Tang, H. Wang, R. Becheker, J.-L. Oudar, D. Gaponov, T. Godin, and A. Hideur, Opt. Lett. **40**, 1414 (2015).
17. I. Pavlov, E. Ilbey, E. Dülgergil, A. Bayri, and F. Ilday, Opt. Express **20**, 9471 (2012).
18. P. Elahi, H. Kalaycıoğlu, H. Li, Ö. Akçaalan, and F. Ilday, Opt. Commun. **403**, 381 (2017).
19. D. A. Gaponov, L. V. Kotov, M. E. Likhachev, M. M. Bubnov, A. Cabasse, J.-L. Oudar, S. Fevrier, D. S. Lipatov, N. N. Vechkanov, A. N. Guryanov, and G. Martel, Opt. Lett. **37**, 3186 (2012).
20. H. Wang, L. V. Kotov, D. A. Gaponov, A. Cabasse, M. V. Yashkov, D. S. Lipatov, M. E. Likhachev, J. Oudar, G. Martel, S. Février, and A. Hideur, IEEE J. Sel. Top. Quantum Electron. **20**, 0903007 (2014).
21. G. Sobon, P. Kaczmarek, D. Sliwinska, J. Sotor, and K. M. Abramski, IEEE J. Sel. Top. Quantum Electron. **20**, 492 (2014).
22. G. Imeshev, I. Hartl, and M. E. Fermann, Opt. Express **12**, 6508 (2004).
23. S. Zhou, F. W. Wise, and D. G. Ouzounov, Opt. Lett. **32**, 871 (2007).
24. A. Klenke, M. Kienel, T. Eidam, S. Hädrich, J. Limpert, and A. Tünnermann, Opt. Lett. **38**, 4593 (2013).
25. F. Guichard, M. Hanna, Y. Zaouter, D. N. Papadopoulos, F. Druon, and P. Georges, IEEE J. Sel. Top. Quantum Electron. **20**, 619 (2014).
26. Q. Hao, Q. Zhang, T. Sun, J. Chen, Z. Guo, Y. Wang, Z. Guo, K. Yang, and H. Zeng, Appl. Phys. Lett. **106**, 101103 (2015).
27. Q. Hao, Y. Wang, T. Liu, H. Hu, and H. Zeng, IEEE Photon. J. **8**, 7101908 (2016).
28. S. Zhou, L. Kuznetsova, A. Chong, and F. W. Wise, Opt. Express **13**, 4869 (2005).